Chapter 1

Results

In order to provide a comprehensive prediction of the sensitivity of the analysis regions to the signal model, we perform an exclusion fit. In an exclusion fit, the signal model plus the standard model background is taken as the null hypothesis and is tested against the alternative hypothesis of the background only model. The following chapter describes the process of the fit, and provides the results.

1.1 Statistical Framework

In each signal region, we create a histogram of all events in the sample that are within the region, consisting of several bins of a chosen variable x. The expectation value for the number of events in a single bin is:

$$E[n_i] = \mu s_i(\boldsymbol{\theta}) + b_i(\boldsymbol{\theta}), \tag{1.1}$$

where μ is the parameter of interest, the signal strength, which is 0 in the background-only case and 1 in the nominal signal model. The vector of variables $\boldsymbol{\theta}$ represents the set of nuisance parameters, and s_i and b_i are the expected number of signal and background events in bin i:

$$\begin{aligned} s_i &= s_{tot} \int_{\text{bin i}} f_s(x|\boldsymbol{\theta})dx \\ b_i &= b_{tot} \int_{\text{bin i}} f_b(x|\boldsymbol{\theta})dx. \end{aligned} \tag{1.2}$$

Here, $f_s(x|\boldsymbol{\theta})$ and $f_b(x|\boldsymbol{\theta})$ are the probability density functions of the variable x for signal and background events. The variables s_{tot} and b_{tot} contain the total mean numbers of signal and background events, where b_{tot} is allowed to vary and s_{tot} is fixed to the value predicted by the MC signal samples. In each control region, we build a similar histogram with a single bin with the expected value:

$$E[m_i] = b_i(\boldsymbol{\theta}). \tag{1.3}$$

We can then construct a likelihood function from the product of Poisson probabilities for each bin:

$$L(\mu, \boldsymbol{\theta}) = C_{sys}(\boldsymbol{\theta}^0, \boldsymbol{\theta}) \prod_{j=1}^{N} \frac{E[n_j]}{n_j!} e^{-E[n_j]} \prod_{k=1}^{M} \frac{E[m_k]}{m_k!} e^{-E[m_k]}, \tag{1.4}$$

where $C_{sys}(\boldsymbol{\theta}^0, \boldsymbol{\theta})$ is a product of probability distributions for the measurements describing each systematic uncertainty. These are taken to be Gaussian distributed, and are each scaled to have unit standard deviations, giving:

$$C_{sys}(\boldsymbol{\theta}^0, \boldsymbol{\theta}) = \prod_{m \in S} G(\boldsymbol{\theta}^0_m - \boldsymbol{\theta}_m, \sigma = 1). \tag{1.5}$$

We then test a hypothesized value of the signal strength μ using the profile log-likelihood ratio as the test statistic:

$$t_\mu = -2 \log \left(\frac{L(\mu_{\text{sig}}, \hat{\hat{\boldsymbol{\theta}}})}{L(\hat{\mu}_{\text{sig}}, \hat{\boldsymbol{\theta}})} \right), \tag{1.6}$$

where $\hat{\hat{\boldsymbol{\theta}}}$ is the set of nuisance parameters which maximize the likelihood function for the chosen signal strength μ_{sig}, and $\hat{\boldsymbol{\theta}}$ and $\hat{\mu}_{\text{sig}}$ are the unconditional maximum-likelihood estimators for L. From this we compute the p-value corresponding to a given signal strength μ_{sig} by integrating the probability distribution of t_μ:

$$p_\mu = \int_{t_{\mu_{\text{obs}}}}^{\infty} f(t_\mu | \mu_{\text{sig}}, \boldsymbol{\theta}) dt_\mu. \tag{1.7}$$

This probability distribution can be estimated by generating toy MC experiments, however in the "asymptotic" regime with sufficiently high statistics (usually at least $\mathcal{O}(5)$ expected signal events) this distribution is known to follow a χ^2 distribution

according to Wilks theorem [4]. Using this p-value formula, we follow the $\mathrm{CL_s}$ technique to present results [3]. We calculate $\mathrm{CL_{s+b}}$ as the p-value for the existence of the signal model with some $\mu_{\mathrm{sig}} > 0$ and $1 - \mathrm{CL_b}$ as the p-value for the background-only case $\mu_{\mathrm{sig}} = 0$:

$$\begin{aligned} \mathrm{CL_{s+b}}(\mu_{\mathrm{sig}}) &= \int_{t_{\mu_{\mathrm{obs}}}}^{\infty} f(t_\mu|\mu_{\mathrm{sig}}, \boldsymbol{\theta}) dt_\mu \\ 1 - \mathrm{CL_b} &= \int_{t_{\mu_{\mathrm{obs}}}}^{\infty} f(t_\mu|0, \boldsymbol{\theta}) dt_\mu. \end{aligned} \tag{1.8}$$

$\mathrm{CL_s}$ is then given by the ratio of these two quantities:

$$\mathrm{CL_s}(\mu_{\mathrm{sig}}) = \frac{\mathrm{CL_{s+b}}(\mu_{\mathrm{sig}})}{1 - \mathrm{CL_b}}. \tag{1.9}$$

To perform an exclusion fit, we evaluate $\mathrm{CL_s}$ for the nominal signal strength $\mu_{\mathrm{sig}} = 1$, and exclude signal models with $\mathrm{CL_s}(1) > 0.05$. We perform this statistical anlysis of the finalized analysis regions using the HistFitter software package [2].

1.2 Minimum m_s

As a discrimination variable for the exclusion fit, we use a partial reconstruction of the s mass. The s can not be fully reconstructed because the E_T^{miss} derived from the neutrino cannot be distinguished from the E_T^{miss} derived from dark matter. Instead, we calculate the minimum possible s mass m_s^{min} consistent with the other measured s decay products. This variable shows good discrimination power, but is not used in the signal region selection because the distribution shape varies widely across signal points according to their s mass.

To calculate m_s^{min} we begin by using the W mass constraint on the charged lepton-neutrino system to solve for the neutrino energy E_ν as a function of the angle $\theta_{\ell\nu}$ between the charged lepton and neutrino:

$$\begin{aligned} E_\nu &= \frac{m_W^2}{2E_l(1 - \cos\ \theta_{l\nu})}, \text{ where} \\ m_W^2 &= (p_l + p_\nu)^2 = 2p_l p_\nu = 2E_l E_\nu (1 - \cos\ \theta_{l\nu}). \end{aligned} \tag{1.10}$$

We then rotate the coordinate system to place the neutrino 3-momentum along the z-axis and the hadronic W (W_H) 3-momentum in the x-z plane. The neutrino 4-

momentum is then:

$$p_\nu = \frac{m_W^2}{2E_l(1-\cos\ \theta_{l\nu})}(\sin\theta_{l\nu}, \sin\theta_{l\nu}\sin\phi_\nu, \cos\theta_{l\nu}, 1). \tag{1.11}$$

We can then write the s mass as:

$$\begin{gathered} m_s^2 = (p_{W_H} + p_l + p_\nu)^2 \\ m_s^2 = (E_{W_H} + E_l + E_\nu)^2 - (p_{W_{Hx}} + E_\nu \sin\theta_{l\nu}\cos\phi_\nu)^2 - (E_\nu \sin\theta_{l\nu}\sin\phi_\nu)^2 \\ -(E_l + p_{W_{Hz}} + E_\nu\cos\theta_{l\nu})^2. \end{gathered} \tag{1.12}$$

It is clear from this equation that m_s is minimized with $\phi_\nu = 0$, and substituting this and Equation 1.10 for E_v we are left with an expression for m_s with $\theta_{l\nu}$ as the only remaining unknown variable:

$$\begin{aligned} m_s^2 = \left(E_l + \frac{m_W^2}{2E_l(1-\cos\ \theta_{l\nu})} + E_{W_H}\right)^2 - \left(|\vec{p_{W_H}}|\sin\theta_{W_l} + \frac{\sqrt{1-\cos^2\theta_{l\nu}}m_W^2}{2E_l(1-\cos\ \theta_{l\nu})}\right)^2 \\ - \left(E_l + |\vec{p_{W_H}}|cos\theta_{W_l} + \frac{\cos\theta_{l\nu}m_W^2}{2E_l(1-\cos\ \theta_{l\nu})}\right)^2. \end{aligned} \tag{1.13}$$

We then vary $\theta_{l\nu}$ on the interval $[0, \pi]$ to search for the minimum m_s. Figure 1.1 shows the signal and background distributions of $m_s^{\min}$ in both signal regions, demonstrating the strong discrimination potential and large variance between signal samples that make it an ideal model fitting variable. During model fitting we place events in 5 equal width bins in the range $125 \leq m_s \leq 375$

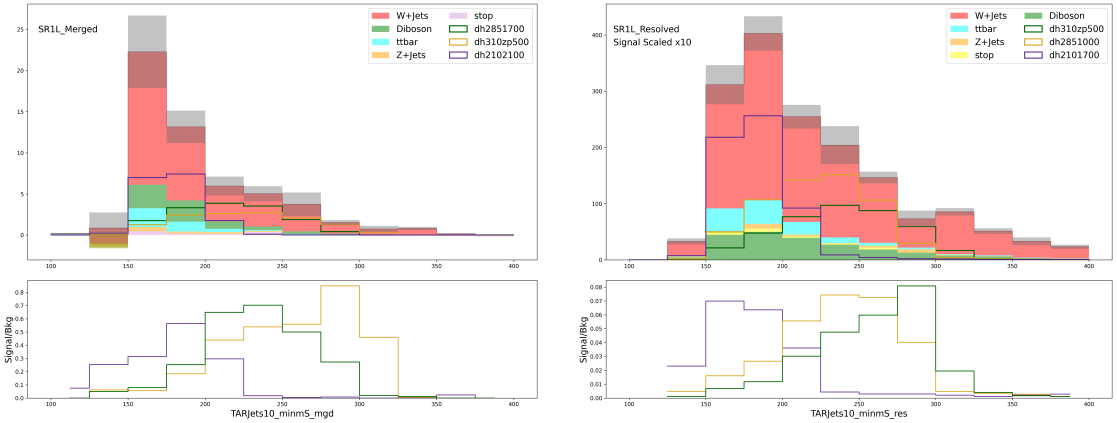

(a) "Merged" SR (b) "Resolved" SR

Figure 1.1: Distributions of $m_s^{\min}$ in the "merged" and "resolved" signal regions.

1.3 Systematic Uncertainties

While statistical fluctuations are uncorrelated between measurements and arise from a measurement consisting of a limited number of observations, systematic uncertainties are often correlated across repeated measurements, generally do not scale with the sample size, and may derive from the nature of the experiment or uncertainty in the model used to make conclusions about the data. For this analysis we further categorize systematic uncertainties into theory uncertainties on the modelling and experimental uncertainties. The evaluation of theory uncertainties on is not within the scope of this thesis, and I assign them a flat value of 20% of the yield on each background category. A short description of the various types of experimental systematic uncertainties considered follows.

1.3.1 $R = 0.4$ Jets

Uncertainties on $R = 0.4$ jets are divided into jet energy scale (JES) and jet energy resolution (JER) uncertainties. These include, but are not limited to, uncertainties on pileup, flavour composition, and punch-through of jets. We evaluate them using tools provided by the ATLAS Jet/E_T^{miss} group.

1.3.2 Track Uncertainties

These are uncertainties on the reconstruction of tracks in the ATLAS inner detector. In this analysis they are primarily propagated into the reconstruction of TAR jets in the "merged" signal and control regions.

1.3.3 Muon and Electron

For muons and electrons we consider uncertainties on the reconstruction efficiency, isolationa and identification, and energy or momentum scale and resolution. We evaluate these uncertainties using tools provided by the ATLAS E/Gamma and Muon combined performance groups.

1.3.4 E_T^{miss}

We propagate uncertainties on the afformentioned objects into the E_T^{miss} calculation, however we consider separate E_T^{miss} systematics which affect the reconstruction of the

E_T^{miss} soft term. We evaluate these using the METSystematicsTool.

1.3.5 Luminosity

The integrated luminosity measured across the run-2 data taking period is known to a precision of 1.7%. This is therefore applied as an overall systematic across the normalization of all MC events.

1.4 Fit Results

1.4.1 Background Only Fit

I first perform a background-only fit to examine the effects of systematic uncertainties and control region normalization on background predictions in the signal regions. The signal regions for this analysis remain blinded; therefore ATLAS data in the signal regions is mimicked by Asimov data with a yield equal to the nearest integer value to the pre-fit total background yield in each bin.

Figures 1.2 and 1.3 show comparisons of the pre-fit and post-fit yields in each region for the background only fit, while Tables 1.1 and 1.2 give a more detailed numerical breakdown. In the "merged" signal region, the fit increases the expected number of SM events primarily due to an increase in expected $W+$jets events from the normalization derived in the "merged" $W+$jets control region. In the "resolved" signal region, the fit decreases the expected background yield, again primarily due to normalization this time from the "resolved" $W+$jets control region. In both cases the uncertainty on the predicted $W+$jets yield is reduced. In both the "merged" and "resolved" categories the $t\bar{t}$ control regions slightly reduce the predicted $t\bar{t}$ yield and substantially reduce the uncertainty on those predictions.

Tables 1.3 and 1.4 summarize the uncertainty on the total yield in each analysis region from statistical and systematic sources. Uncertainties preceded by "μ", "α", and "γ" represent normalization, systematic, and statistical uncertainties respectively. The leading sources of uncertainty in both signal regions are normalization factors and theory uncertainties on the $W+$jets background, followed by a mix of JER experimental systematics and bin-by-bin statistical uncertainties.

Category	SR_Merged	CRW_Merged	CRTT_Merged
Observed events	59	314	68
Fitted SM events	63.36 ± 11.40	313.99 ± 17.67	67.99 ± 8.23
Fitted Diboson events	7.65 ± 1.77	40.65 ± 9.11	0.16 ± 0.04
Fitted WJets events	48.69 ± 10.73	242.14 ± 21.10	0.26 ± 0.16
Fitted ttbar events	3.37 ± 0.64	12.93 ± 2.32	61.47 ± 8.35
Fitted ZJets events	1.16 ± 0.27	12.06 ± 3.22	0.00 ± 0.00
Fitted stop events	1.30 ± 0.49	3.30 ± 0.81	6.08 ± 1.35
MC exp. SM events	59.91 ± 13.16	295.80 ± 58.00	84.89 ± 16.12
MC exp. Diboson events	7.65 ± 1.78	40.65 ± 9.16	0.16 ± 0.04
MC exp. WJets events	44.31 ± 12.16	220.38 ± 53.40	0.24 ± 0.15
MC exp. ttbar events	4.30 ± 1.02	16.49 ± 3.81	78.40 ± 16.02
MC exp. ZJets events	1.16 ± 0.27	12.06 ± 3.24	0.00 ± 0.00
MC exp. stop events	1.30 ± 0.49	3.30 ± 0.82	6.08 ± 1.36

Table 1.1: Pre and post-fit yields for each background category in the merged signal and control regions for a background-only fit.

Category	SR_Resolved	CRW_Resolved	CRTT_Resolved
Observed events	1655	1750	499
Fitted SM events	1460.37 ± 112.58	1749.98 ± 41.87	498.88 ± 22.31
Fitted Diboson events	204.53 ± 42.06	240.35 ± 49.79	2.88 ± 0.61
Fitted WJets events	1043.56 ± 109.95	1309.19 ± 69.50	$3.80^{+5.62}_{-3.80}$
Fitted ttbar events	131.89 ± 10.37	82.38 ± 6.58	449.84 ± 24.75
Fitted ZJets events	52.83 ± 11.17	89.82 ± 18.33	2.30 ± 0.47
Fitted stop events	17.92 ± 4.30	17.50 ± 3.68	39.99 ± 8.22
MC exp. SM events	1655.04 ± 299.65	1993.57 ± 335.94	503.10 ± 95.22
MC exp. Diboson events	204.52 ± 42.33	240.35 ± 50.12	2.88 ± 0.61
MC exp. WJets events	1237.19 ± 286.11	1552.13 ± 325.02	$4.50^{+6.90}_{-4.50}$
MC exp. ttbar events	132.92 ± 27.85	83.02 ± 17.13	453.35 ± 93.13
MC exp. ZJets events	52.83 ± 11.24	89.82 ± 18.45	2.30 ± 0.48
MC exp. stop events	17.92 ± 4.33	17.50 ± 3.71	39.99 ± 8.27

Table 1.2: Pre and post-fit yields for each background category in the resolved signal and control regions for a background-only fit.

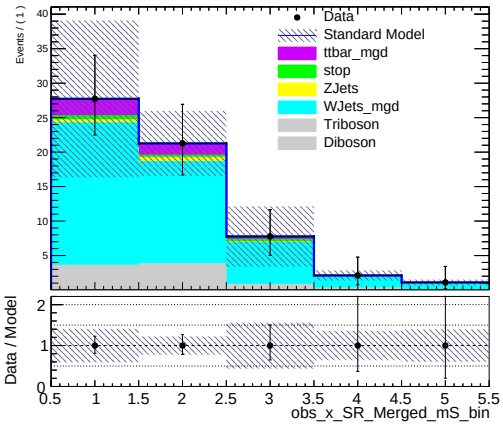

(a) Merged SR pre-fit

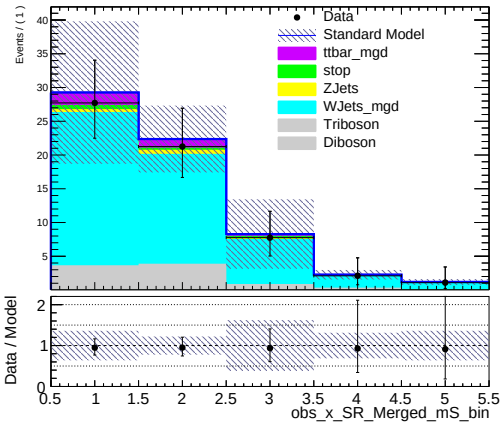

(b) Merged SR post-fit

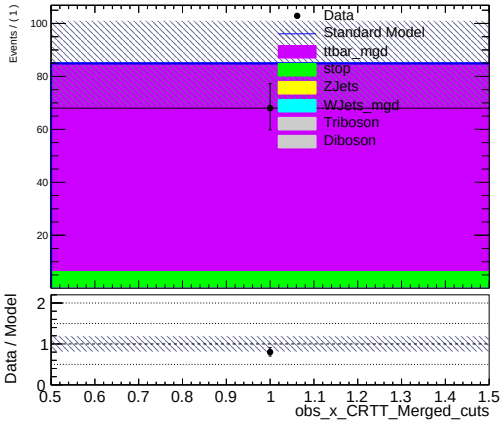

(c) Merged CR $t\bar{t}$ pre-fit

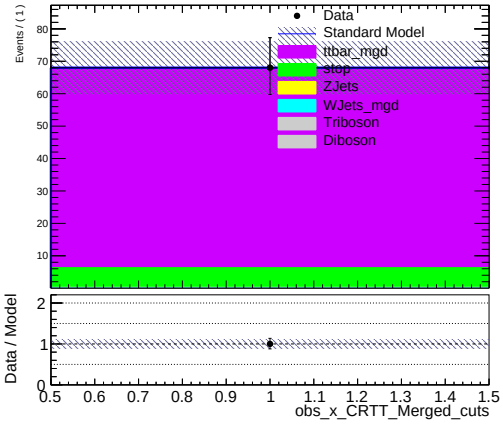

(d) Merged CR $t\bar{t}$ post-fit

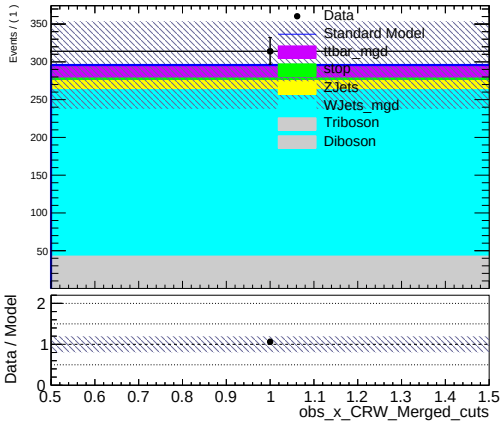

(e) Merged CR W+jets pre-fit

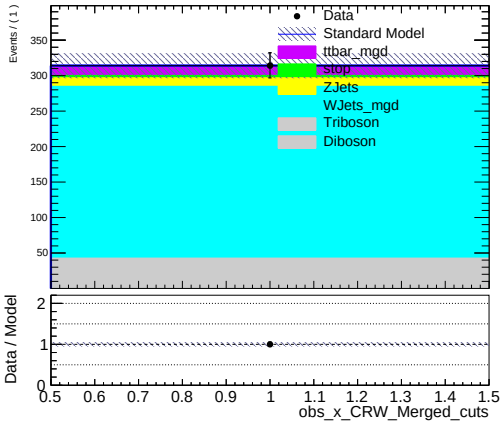

(f) Merged CR W+jets post-fit

Figure 1.2: Pre and post-fit yields in the merged signal and control regions for a background-only fit.

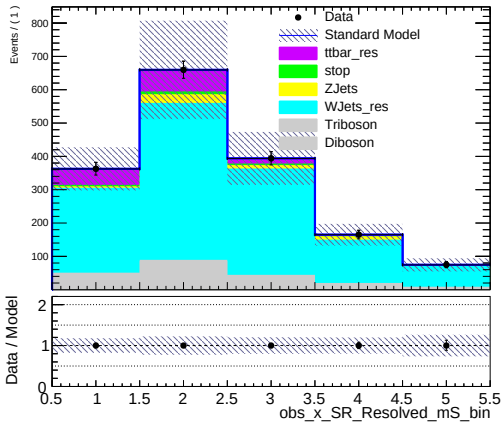

(a) Resolved SR pre-fit

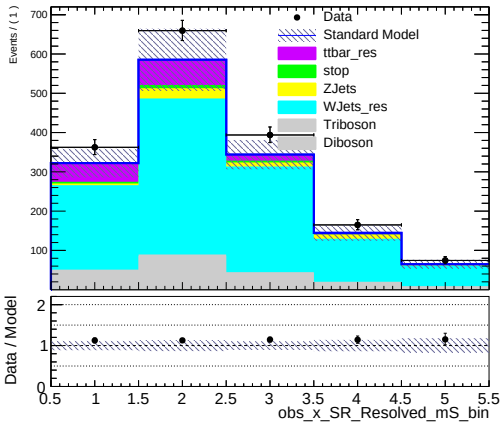

(b) Resolved SR post-fit

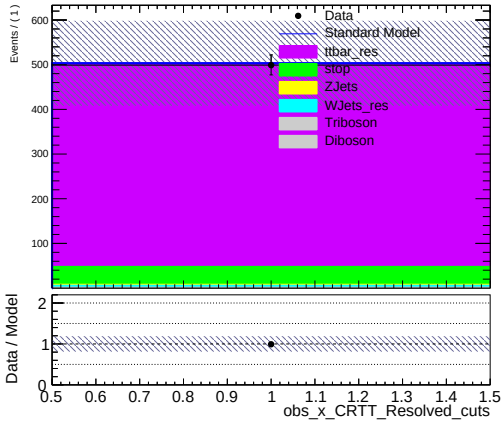

(c) Resolved CR $t\bar{t}$ pre-fit

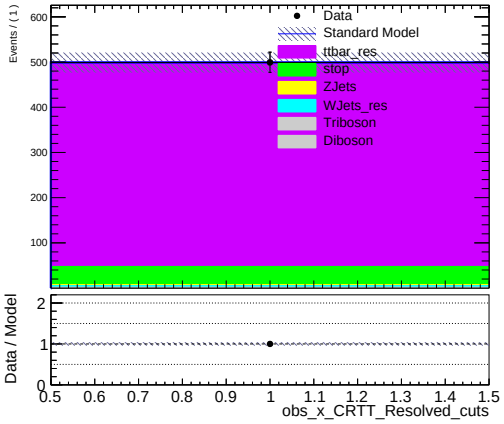

(d) Resolved CR $t\bar{t}$ post-fit

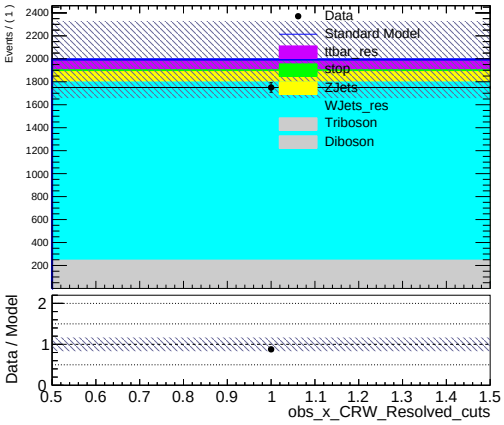

(e) Resolved CR W+jets pre-fit

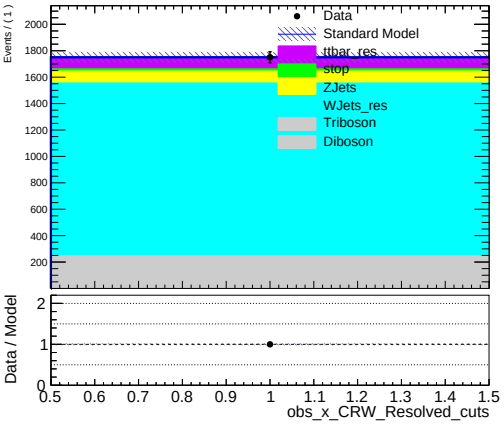

(f) Resolved CR W+jets post-fit

Figure 1.3: Pre and post-fit yields in the resolved signal and control regions for a background-only fit.

Uncertainty	SR_Merged	CRW_Merged	CRTT_Merged
Total background expectation	63.36	313.99	67.99
Total statistical ($\sqrt{N_{\text{exp}}}$)	±7.96	±17.72	±8.25
Total background systematic	±11.40 [18.00%]	±17.67 [5.63%]	±8.23 [12.11%]
μ_Wjets_mgd	±13.15	±65.39	±0.07
α_WJetsTheorySys	±9.69	±48.18	±0.05
γ_stat_SR_Merged_mS_Bin0	±5.22	±0.00	±0.00
α_JET_Flavor_Composition	±4.70	±11.80	±0.33
γ_stat_SR_Merged_mS_Bin1	±3.54	±0.00	±0.00
α_JET_Flavor_Response	±3.27	±15.54	±1.01
α_MET_SoftTrk_ResoPerp	±3.10	±1.68	±0.00
α_JET_Pileup_OffsetNPV	±2.34	±2.30	±0.01
α_JET_EtaIntercalibration	±1.89	±2.81	±0.40
α_MET_SoftTrk_Scale	±1.81	±0.86	±0.09
α_MET_SoftTrk_ResoPara	±1.69	±0.00	±0.46
γ_stat_SR_Merged_mS_Bin2	±1.66	±0.00	±0.00
α_DibosonTheorySys	±1.52	±8.08	±0.03
α_JET_Pileup_PtTerm	±1.20	±3.35	±0.72
α_lumiSys	±1.07	±5.30	±1.15
α_JET_Pileup_RhoTopology	±0.95	±5.00	±0.34
μ_ttbar_mgd	±0.83	±3.18	±15.10
α_JET_EffectiveNP_Modelling1	±0.71	±7.75	±0.13
α_ttbarTheorySys	±0.67	±2.56	±12.16

Table 1.3: Effect of systematic uncertainties in the merged signal and control regions for a background-only fit. Uncertainties with a magnitude <1% of total yield are excluded.

Uncertainty	SR_Resolved	CRW_Resolved	CRTT_Resolved
Total background expectation	1460.37	1749.98	498.88
Total statistical ($\sqrt{N_{\text{exp}}}$)	±38.21	±41.83	±22.34
Total background systematic	±112.58 [7.71%]	±41.87 [2.39%]	±22.31 [4.47%]
μ_Wjets_res	±230.37	±289.01	±0.84
α_WJetsTheorySys	±207.62	±260.47	±0.76
α_JET_Flavor_Composition	±73.19	±42.72	±7.29
α_JET_Pileup_RhoTopology	±70.72	±17.17	±5.99
α_JET_Flavor_Response	±58.20	±49.70	±13.63
α_DibosonTheorySys	±40.64	±47.76	±0.57
γ_stat_SR_Resolved_mS_Bin1	±33.27	±0.00	±0.00
γ_stat_SR_Resolved_mS_Bin2	±29.72	±0.00	±0.00
γ_stat_SR_Resolved_mS_Bin0	±28.50	±0.00	±0.00
μ_ttbar_res	±28.35	±17.71	±96.70
α_MET_SoftTrk_ResoPerp	±26.81	±0.22	±11.19
α_ttbarTheorySys	±26.08	±16.29	±88.95
α_lumiSys	±24.66	±29.55	±8.42
α_JET_EffectiveNP_Modelling1	±22.19	±18.10	±5.48

Table 1.4: Effect of systematic uncertainties in the resolved signal and control regions for a background-only fit. Uncertainties with a magnitude <1% of total yield are excluded.

1.4.2 Exclusion Fit

I finally perform an exclusion fit using the signal model. I evaluate the CL_s for the nominal signal strength $\mu_{sig} = 1$ for each signal mass point in the m_s-$m_{Z'}$ plane, and interpolate between mass points using a cubic interpolation. The signal regions remain blinded, so I once again replace ATLAS data with Asimov data equal to the nearest integer value to the pre-fit MC expected SM yield in those regions. I then build a contour along $CL_s = 0.05$, and the area outside this contour ($CL_s > 0.05$) would be excluded at a 95% confidence level with the Asimov data. This provides the strongest estimate of the designed regions' sensitivity to the dark Higgs signal model prior to unblinding.

I first perform an exclusion fit on the "merged" analysis channel alone to assess the sensitivity of the "merged" signal region selection criteria I designed. The expected exclusion contour for the "merged" channel is shown in Figure 1.4. I then perform an exclusion fit of the "resolved" channel alone, with the expected exclusion contour shown in Figure 1.5 to see how it complements the "merged" channel. Finally, in Figure 1.6 I show the expected exclusion contour for the combined "merged" and "resolved" channels, demonstrating the full expected exclusion power of the analysis. Figure 1.7 shows the expected and observed exclusion limits obtained in the fully hadronic $s \to WW$ decay channel for comparison.

The expected exclusion contours show that the merged region dominates sensitivity, and that we expect to substantially improve on the limits set in the fully hadronic decay channel in our analysis.

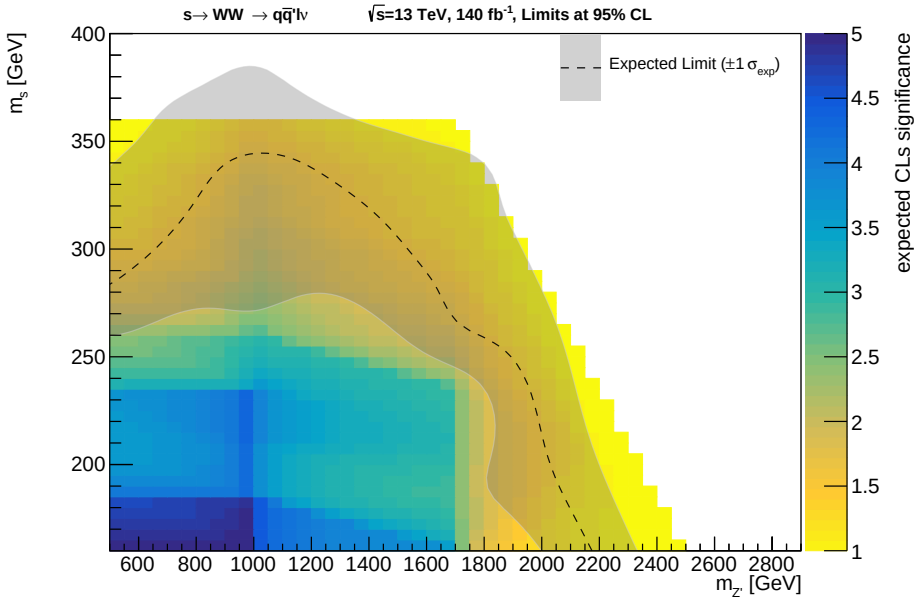

Figure 1.4: Expected exclusion limits for the dark Higgs signal model obtained using the "merged" signal and control regions.

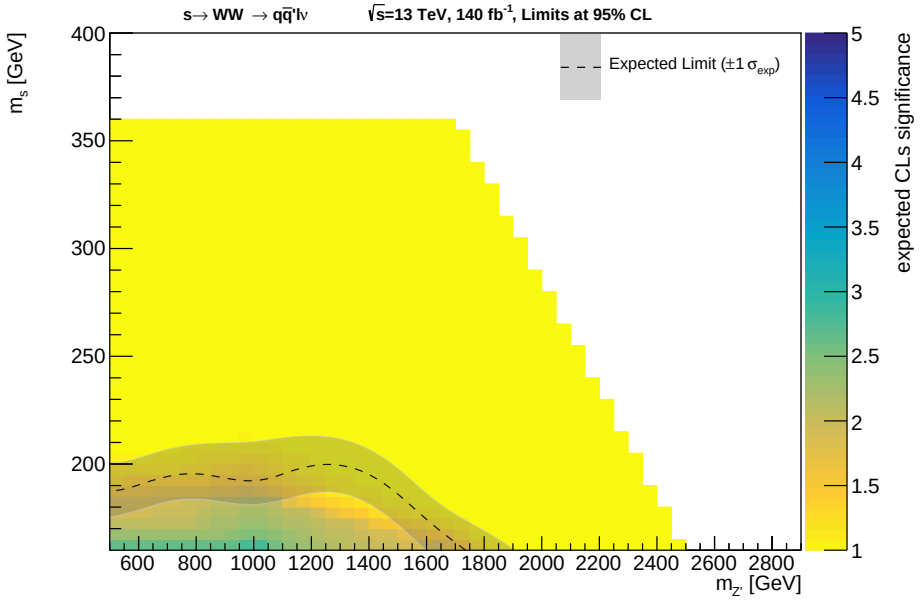

Figure 1.5: Expected exclusion limits for the dark Higgs signal model obtained using the "resolved" signal and control regions.

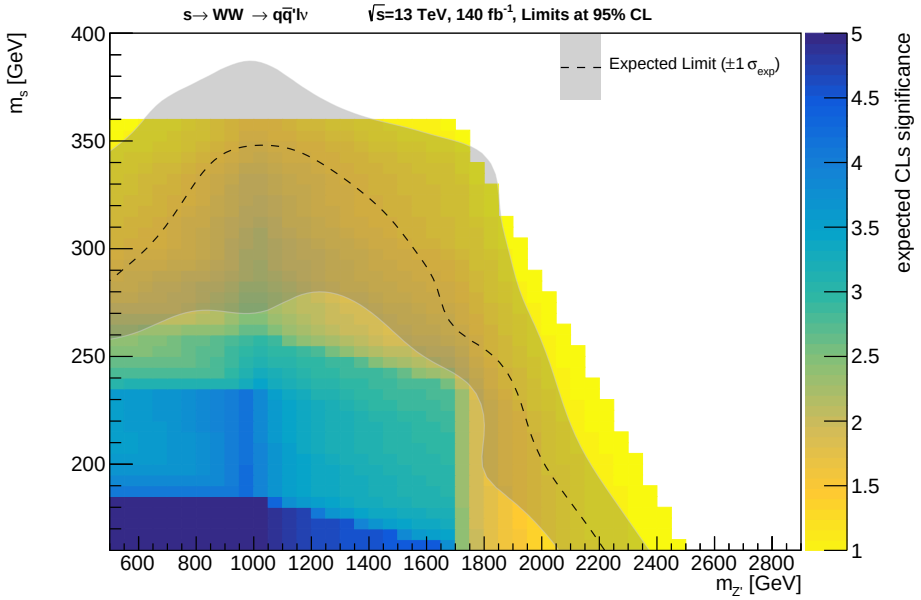

Figure 1.6: Expected exclusion limits for the dark Higgs signal model obtained using the "merged" and "resolved" signal and control regions.

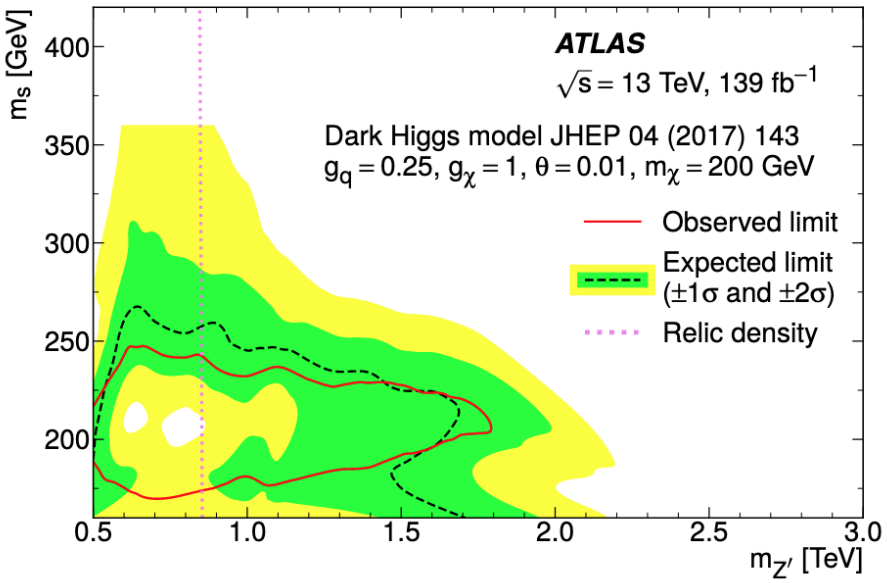

Figure 1.7: Expected and observed exclusion limits for the dark Higgs signal model from the fully hadronic $s \to WW$ channel from [1].

Bibliography

[1] Georges Aad et al. "Search for Dark Matter Produced in Association with a Dark Higgs Boson Decaying into $W^{\pm}W^{\mp}$ or ZZ in Fully Hadronic Final States from $\sqrt{s} = 13\,\text{TeV}$ pp Collisions Recorded with the ATLAS Detector". In: *Phys. Rev. Lett.* 126.12 (2021), p. 121802. DOI: 10.1103/PhysRevLett.126.121802. arXiv: 2010.06548 [hep-ex].

[2] M. Baak et al. "HistFitter software framework for statistical data analysis". In: *Eur. Phys. J. C* 75 (2015), p. 153. DOI: 10.1140/epjc/s10052-015-3327-7. arXiv: 1410.1280 [hep-ex].

[3] A L Read. "Presentation of search results: theCLstechnique". In: *Journal of Physics G: Nuclear and Particle Physics* 28.10 (2002), pp. 2693–2704. DOI: 10.1088/0954-3899/28/10/313. URL: https://doi.org/10.1088/0954-3899/28/10/313.

[4] S. S. Wilks. "The Large-Sample Distribution of the Likelihood Ratio for Testing Composite Hypotheses". In: *The Annals of Mathematical Statistics* 9.1 (1938), pp. 60 –62. DOI: 10.1214/aoms/1177732360. URL: https://doi.org/10.1214/aoms/1177732360.